Intense plasma wave emissions associated with Saturn's moon Rhea

O. Santolík,[1,2,3] D. A. Gurnett,[1] G. H. Jones,[4] P. Schippers,[1] F. J. Crary,[5] J. S. Leisner,[1] G. B. Hospodarsky,[1] W. S. Kurth,[1] C. T. Russell,[6] and M. K. Dougherty[7]

Received 5 August 2011; revised 3 September 2011; accepted 6 September 2011; published 11 October 2011.

[1] Measurements by the Cassini spacecraft during a close flyby of Saturn's moon Rhea on March 2, 2010, show the presence of intense plasma waves in the magnetic flux tube connected to the surface of the moon. Three types of waves were observed, (1) bursty electrostatic waves near the electron plasma frequency, (2) intense whistler-mode emissions below one half of the electron cyclotron frequency, and (3) broadband electrostatic waves at frequencies well below the ion plasma frequency. The waves near the electron plasma frequency are believed to be driven by a low energy (~35 eV) electron beam accelerated away from Rhea. Their bursty structure is believed to be due to a nonlinear process similar to the three-wave interaction that occurs for Langmuir waves in the solar wind. The whistler-mode emissions are propagating toward Rhea and are shown to be generated by the loss-cone anisotropy (at parallel cyclotron resonance energies around 230 eV) caused by absorption of electrons at the surface of the moon. Scattering by these whistler-mode waves may be able to explain previously reported depletions of energetic electrons in the vicinity of the moon. The low-frequency waves may play a role in nonlinear three-wave interactions with the bursty electrostatic waves. **Citation:** Santolík, O., D. A. Gurnett, G. H. Jones, P. Schippers, F. J. Crary, J. S. Leisner, G. B. Hospodarsky, W. S. Kurth, C. T. Russell, and M. K. Dougherty (2011), Intense plasma wave emissions associated with Saturn's moon Rhea, *Geophys. Res. Lett.*, *38*, L19204, doi:10.1029/2011GL049219.

1. Introduction

[2] Saturn's largest icy moon Rhea orbits at a distance of 8.7 R_S (Saturn's radii) from the center of the planet. Its internal geological activity is negligible [*Pitman et al.*, 2008] and the passive interaction of the moon with Saturn's magnetosphere is believed to be the source of its tenuous oxygen–carbon dioxide atmosphere [*Teolis et al.*, 2010]. Although Saturn's magnetosphere has only minor effects on the moon, Rhea strongly modifies the properties of the magnetospheric plasma in its vicinity [*Wilson et al.*, 2010]. During the November 26, 2005 Cassini flyby of Rhea, a depletion of energetic electrons has been observed within several radii of the moon. *Jones et al.* [2008] suggested that the depletion is caused by a disk of absorbing debris around Rhea, possibly in the form of discrete rings or arcs of material. This hypothesis is not consistent with direct optical observations which revealed no evidence of such material [*Tiscareno et al.*, 2010]. No other explanation of the surprising depletions of electrons has been found so far. Interactions of the energetic electrons with various types of waves occurring in the magnetospheric plasma may play a role in the loss process causing these depletions. The purpose of this paper is to investigate the wave environment of Rhea in connection with properties of electron phase space density distributions and magnetic field. We discuss the generation mechanisms of the observed waves and their possible effects on energetic electrons.

2. Wave Environment of Rhea

[3] Measurements by the Cassini Radio and Plasma Wave instrument [*Gurnett et al.*, 2004] during the March 2, 2010, close flyby of Rhea (Figure 1a) reveal that the moon generates a large variety of electrostatic and electromagnetic plasma waves (Figure 1d) that have important implications for the magnetospheric interactions occurring near the moon. Three types of plasma waves were observed; (1) Strong bursty emissions near the electron plasma frequency at 15–20 kHz; (2) Strong whistler-mode emissions below one half of the electron cyclotron frequency at 70 to 250 Hz; (3) Broadband electrostatic waves below about 40 Hz. These waves all occurred from about 1739 to 1742 UT, as the spacecraft passed through the magnetic flux tube connected to the surface of Rhea.

[4] The emissions around 15–20 kHz are at the same frequency as emissions near the electron plasma frequency in the surrounding magnetosphere of Saturn, but six orders of magnitude stronger. These waves are not accompanied by magnetic fluctuations and form wave packets (Figures 1b and 1c), similar to Langmuir waves in the Solar wind and foreshock regions [*Gurnett et al.*, 1993]. The waves between 70 Hz and 250 Hz (~0.1–0.4 of the electron cyclotron frequency) have a significant component of magnetic fluctuations (Figures 1e–1g) and are very similar to whistler-mode chorus emissions which are able to interact with energetic electrons [*Horne et al.*, 2005], causing their diffusion in velocity space. The waves observed at frequencies below 40 Hz (below ~0.1 of the proton plasma frequency) have no magnetic field component and are purely electrostatic (Figure 1h and 1i). Their amplitude abruptly decreases when the spacecraft moves away from the influence of the moon.

3. Plasma Environment of Rhea

[5] The observed electric and magnetic wave fields are clearly caused by plasma instabilities induced by Rhea. To understand the origin of the waves we have investigated the

[1]Department of Physics and Astronomy, University of Iowa, Iowa City, Iowa, USA.
[2]Institute of Atmospheric Physics, Prague, Czech Republic.
[3]Faculty of Mathematics and Physics, Charles University, Prague, Czech Republic.
[4]Mullard Space Science Laboratory and Centre for Planetary Sciences, University College London, Holmbury St. Mary, UK.
[5]Southwest Research Institute, San Antonio, Texas, USA.
[6]Institute of Geophysics and Planetary Physics, University of California, Los Angeles, California, USA.
[7]Blackett Laboratory, Imperial College London, London, UK.

0094-8276/11/2011GL049219

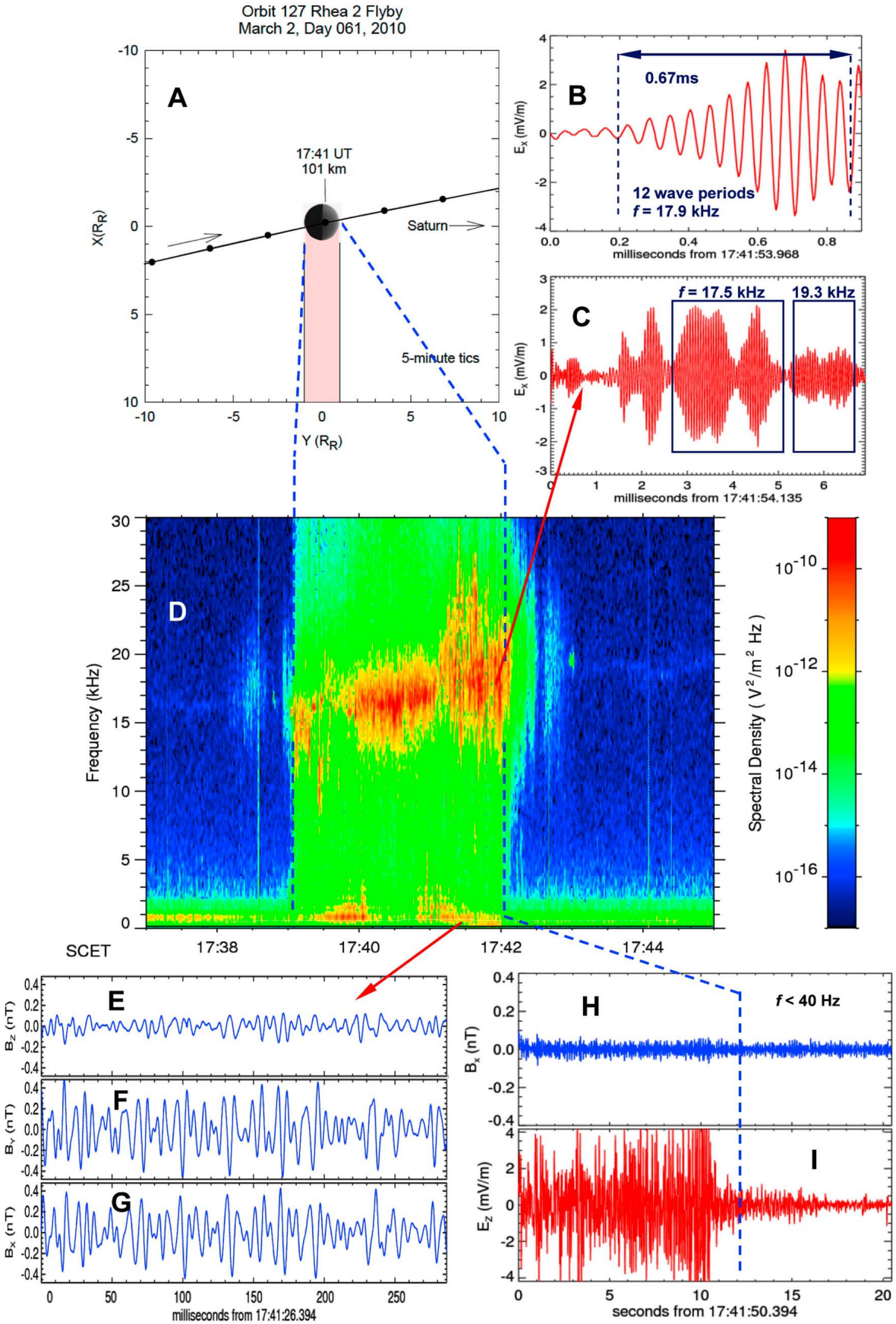
Orbit 127 Rhea 2 Flyby
March 2, Day 061, 2010
A
17:41 UT
101 km
Saturn
5-minute tics
X(R_R)
Y (R_R)
B
0.67ms
12 wave periods
f = 17.9 kHz
E_x (mV/m)
milliseconds from 17:41:53.968
C
f = 17.5 kHz
19.3 kHz
E_x (mV/m)
milliseconds from 17:41:54.135
D
Frequency (kHz)
SCET
17:38
17:40
17:42
17:44
Spectral Density (V²/m² Hz)
E
F
G
B_Z (nT)
B_Y (nT)
B_X (nT)
milliseconds from 17:41:26.394
H
f < 40 Hz
B_x (nT)
I
E_Z (mV/m)
seconds from 17:41:50.394

Figure 1

electron measurements obtained from the Cassini Plasma Spectrometer [*Young et al.*, 2004]. Energy-time dynamic spectrograms of counts per accumulation from 4 selected anodes (out of 8) of the instrument in 63 logarithmic energy steps are shown in Figures 2a–2d. The accumulation time is 23.4 ms per energy step. The data reveal that the moon strongly modifies the electron velocity distributions. During the time interval for which we detect the fluctuating electromagnetic fields, we observe two distinct changes: (1) the electrons at energies above approximately 0.1–1 keV disappear in the direction coming from Rhea, presumably due to absorption by the moon, and (2) a dense electron beam coming from Rhea occurs at energies of 20–100 eV (G. H. Jones, et al., manuscript in preparation, 2011).

[6] We can note in Figures 1 and 2 that both the strong fluctuating electric and magnetic fields and the unstable features in the electron distributions occur and disappear at the same time. The time interval during which unstable features in the electron distributions occur corresponds to the passage of the spacecraft through the magnetic flux tube connected to the Rhea surface. Significant effects on electrons are not expected from the plasma corotation [*Wilson et al.*, 2010], from the spacecraft orbital motion, from the orbital motion of Rhea, nor from the finite Larmor radius. The observed unstable features in the electron distributions between 20 eV and 10 keV should therefore map along the magnetic field lines with an accuracy better than 3% of the radius of Rhea. This mapping is confirmed by measurements of the Cassini fluxgate magnetometer [*Dougherty et al.*, 2004] shown in Figure 3. The measurements also reveal that the magnetic field intensity is 10% stronger above the moon. This increase of the magnetic pressure is consistent with previous measurements in the Rhea wake [*Jones et al.*, 2008; *Khurana et al.*, 2008] which have been explained by a localized decrease of the plasma pressure. The same explanation can be used here for the observed effects in the flux tube above the absorbing body of the moon. Additionally, we observe a field-aligned current system related to Rhea. It can be roughly modeled by a homogeneous current density of -4 nA/m^2 (directed from Rhea) inside the flux tube. The total integrated current from this model is 7.4 kA. At the boundary of the Rhea flux tube, the model doesn't accurately predict the measured magnetic field. As the variations are spiky, larger localized current densities reaching a few tens of nA/m^2 can be expected here.

4. Bursty High-Frequency Electrostatic Waves

[7] Waves near the electron plasma frequency are known to be driven by electron beams [*Gurnett and Bhattacharjee*, 2005]. The electron beam at ~35 eV shown in Figure 2f (its origin is analyzed by Jones et al. (manuscript in preparation, 2011)) is dense and cold enough to cause a positive slope in the reduced electron distribution function (Figure 2i),

$$F(v_{\|}) = 2\pi \int f(v_{\|}, v_{\perp}) v_{\perp}\, d\, v_{\perp}. \quad (1)$$

We obtain $\partial F/\partial\, v_{\|} \sim 2 \times 10^{-8}$ m^{-5}s^2 in the direction antiparallel to the ambient magnetic field (Figure 2h) at a parallel velocity $v_{\|} = v_{\|\mathrm{P}} \sim -0.01c$. This feature is unstable to the Landau resonance [*Gurnett et al.*, 1993] and can generate waves in various modes, for example the Langmuir waves or obliquely propagating upper-hybrid waves. This is similar to the situation that produces type III radio emissions in the Solar wind [*Reiner et al.*, 1995] where the instability in most cases causes a very rapid dissipation of the beam energy into unstable plasma waves, leading to observations of only marginally unstable 'plateau' distributions with $\partial F/\partial\, v_{\|} \sim 0$. However, similar electron distributions with $\partial F/\partial\, v_{\|} > 0$ have been already observed in the solar wind, in connection with the type III radio bursts [*Lin et al.*, 1986]. These distributions are consistent with our observations of very intense plasma fluctuations (see Figures 1b–1d). The Landau-unstable parallel wave numbers for $v_{\|} = v_{\|\mathrm{P}}$ are

$$k_{\|\mathrm{P}} = 2\pi f / v_{\|\mathrm{P}}, \quad (2)$$

where f is the wave frequency. With $f \sim 18$ kHz we obtain $k_{\|\mathrm{P}} \sim -3.8 \times 10^{-2}$ m^{-1}. The corresponding parallel wavelength is then $L_{\|\mathrm{P}} \sim 170$ m, i.e., much larger than the Debye length of the core electron component (assuming a temperature of ~20 eV we obtain $\lambda_{\mathrm{D}} \sim 17$m).

[8] Waves in Figure 1d show very broad-band frequency spectra. This spectral broadening could be hypothetically caused by the Doppler shift Δf resulting from the plasma corotation velocity $v_{\mathrm{c}} = 57$ km/s [*Wilson et al.*, 2010] and a random perpendicular component of the wave vector $k_{\perp}$,

$$2\pi\, \Delta f \sim v_c\, k_{\perp}. \quad (3)$$

For the observed $\Delta f \sim 5$ kHz, we would, however, need unrealistically large values of $k_{\perp} \sim 0.6$ m^{-1}, for which the wavelengths would fall below the Debye length. A plausible explanation of the observed large bandwidth therefore is the presence of short-duration wave packets, documented in Figures 1b and 1c. They indicate the presence of local nonlinear microphysical processes; for example, three-wave interactions can link the low frequency ion acoustic waves, as

Figure 1. Electrostatic and electromagnetic waves observed during the Cassini flyby of Rhea on 2 March 2010. (a) Orbit of the spacecraft with 5-minute ticks, projected on Rhea's orbital plane from the North. Rhea is in the center, the direction to Saturn is to the right, and the wake of corotating cold plasma extends to the bottom. The closest approach altitude of 101 km occurred at 17:41 UT. (b, c) Electric field waveforms measured by the Cassini Radio and Plasma Wave instrument (6) above Rhea, showing distinctly separate wave packets of plasma oscillations. (d) Frequency-time power spectrogram of the electric field fluctuations. Their level increases remarkably between 17:39:05 to 17:42:02, where strong plasma oscillations occur, accompanied at lower frequencies by electron cyclotron harmonic waves, whistler-mode waves and acoustic emissions. (e, f, g) Waveforms of three components of the magnetic field (B_X, B_Y, and B_Z) at frequencies below 2.5 kHz, recorded on March 2, 2010 from 17:41:26.39 UT. The angles between the antenna directions and the static magnetic field $\mathbf{B_0}$ are: 16 degrees for the B_Z-antenna, 86 degrees for the B_Y-antenna, and 74 degrees for the B_X-antenna. (h) Fluctuating magnetic and (i) electric fields at frequencies below 40 Hz recorded around the exit of the spacecraft from the region influenced by Rhea.

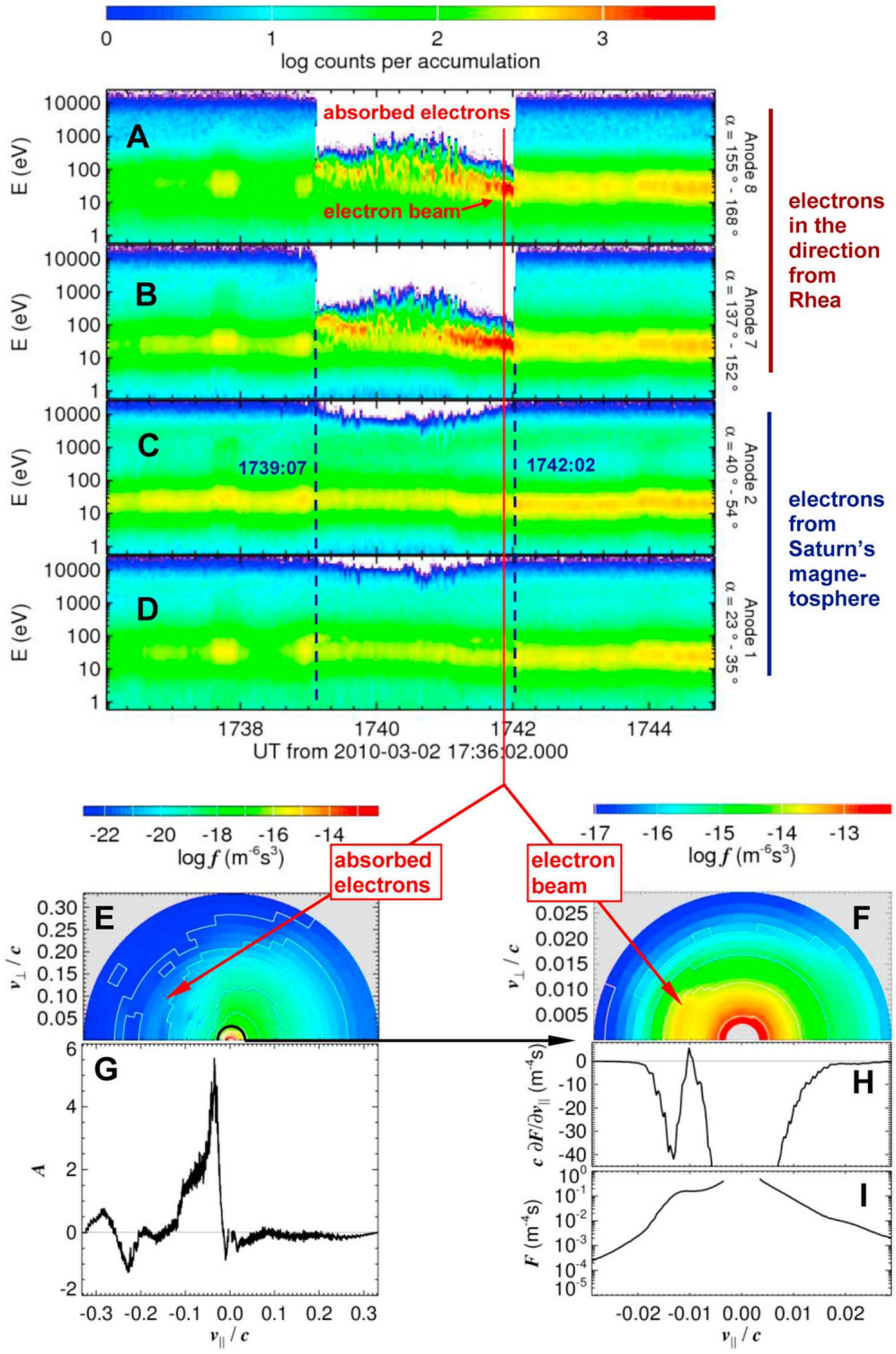

Figure 2. Electrons at energies below 26 keV observed during the Rhea flyby by the Cassini Plasma Spectrometer (9). (a) An energy-time dynamic spectrogram showing counts of electrons in the direction inclined from Saturn's magnetic field by a pitch angle α of 155°–168°, i.e., coming from the direction of Rhea. (b) The same for the neighboring α interval of 137°–152°. (c) The same for α of 40°–54°. (d) The same for α of 23°–35°, i.e., coming from the Saturn's magnetosphere. (e) The phase space density as a function of the velocity components perpendicular and parallel to the ambient magnetic field normalized by the speed of light; arrow shows the region of absorbed electrons at negative parallel velocities. (f) The detail of the phase space density at low electron speeds in the same coordinates; arrow shows the electron beam at negative parallel velocities, i.e. coming from the Rhea direction. (g) The anisotropy as a function of the parallel velocity normalized by the speed of light. (h) The parallel derivative of the one-dimensional reduced distribution. (i) The reduced distribution.

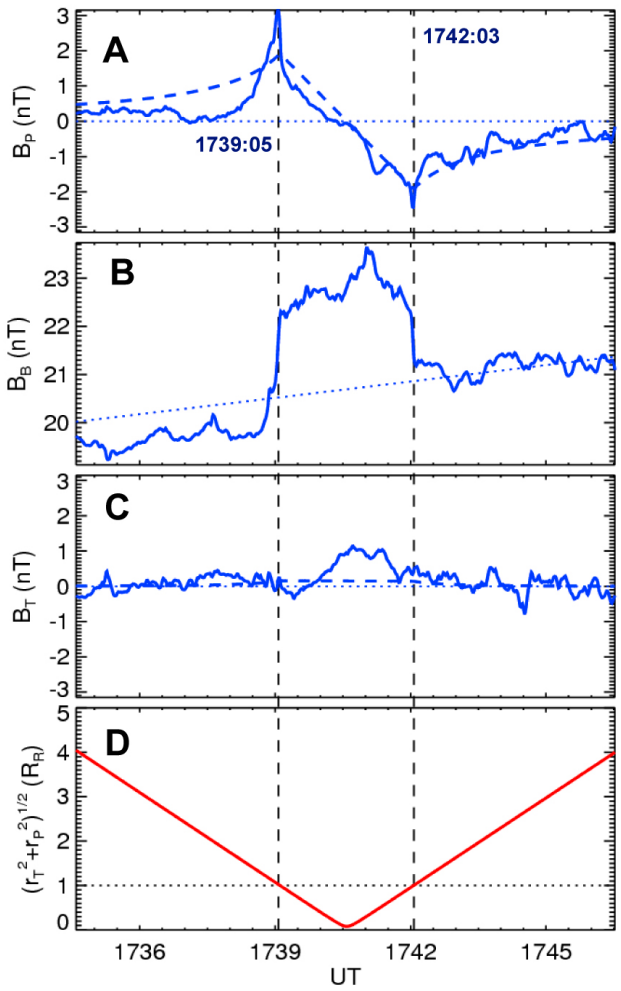

Figure 3. Magnetic field and field aligned currents near Rhea in the *B-P-T* coordinates. The coordinates are constructed from the ambient field estimated by a linear fit of magnetic field components between 17:26 and 17:56 (shown as dotted lines); *B* is along the ambient field direction, *T* is in the plane defined by the direction of the spacecraft orbital velocity and the ambient field direction, and *P* completes the orthogonal set. (a) Component B_P of the magnetic field perpendicular to the ambient field and the spacecraft orbital velocity. The model of a homogeneous current density $i_B = -4$ nA/m^2 inside the Rhea flux tube is shown by a blue dashed line. The positions of the positive and negative peaks are drawn by black vertical dashed lines. (b) Component B_B of the magnetic field along the ambient field direction. (**Cc** Component B_T of the magnetic field in the plane defined by the spacecraft orbit. (d) Distance of Cassini from the Rhea centre measured in the plane perpendicular to the ambient field.

those observed in Figure 1i, with bursty, impulsive plasma oscillations [*Robinson et al.*, 1993] observed in Figures 1b–1d.

5. Whistler-Mode Waves

[9] Detailed wideband waveform measurements were made of the electric and magnetic fields at frequencies below 2.5 kHz where the whistler-mode waves occur. These waveforms are recorded in short snapshots of 2048 samples separated by long gaps of 48 s. One of these snapshots has been taken during 287 ms after 17:41:26.394 UT, in the final part of the Cassini passage through the Rhea magnetic flux tube. Figures 1e–1g show the waveforms measured by three orthogonal magnetic antennas. The B_Z antenna is at a small angle from the background magnetic field $\mathbf{B_0}$, while the B_X and B_Y antennas are nearly perpendicular to $\mathbf{B_0}$. The amplitudes of the measured B_X and B_Y components reach 0.4–0.5 nT. This is approximately 2% of the strength $|\mathbf{B_0}|$ which is 22.9 nT at the time of the waveform measurements. Compared to the amplitudes measured by the B_Z antenna, the B_X and B_Y amplitudes are approximately 3 times larger. This difference implies the presence of electromagnetic waves propagating with wave vectors at small angles from $\mathbf{B_0}$.

[10] Based on these measurements, we have performed a comprehensive polarization and propagation analysis of the observed waves. The three measured orthogonal components of the wave magnetic field have been transformed into a reference frame linked to the $\mathbf{B_0}$ direction. The analysis has been done in the frequency domain, where a broad peak of wave power is observed in Figure 4a at frequencies between 70 and 250 Hz which is between 0.1 and 0.4 of the electron cyclotron frequency ($f_{ce} = 641$ Hz at the time of the waveform measurements).

[11] We have used the singular value decomposition (SVD) method [*Santolík et al.*, 2003] to analyze the magnetic-field polarization ellipsoid. The ratio of its two largest axes, plotted as Ellipticity in Figure 4g, is close to 1 which means a nearly circular polarization. The sign of this value is derived from the phase difference between the components along the two largest axes of the polarization ellipsoid, positive values mean right-handed polarization. These results show that the waves are propagating in the whistler mode. The smallest axis of the polarization ellipsoid is parallel to the wave vector. The angle θ_{KB} in Figure 4e shows that the waves propagate with wave vectors at angles less than 20° with respect to the $\mathbf{B_0}$ direction. The sign of the $\mathbf{B_0}$-component of the Poynting vector [*Santolík et al.*, 2001] has been obtained from the three magnetic antennas and two electric antennas (Figure 4i). It shows positive values indicative of an energy flow from the Saturn's magnetosphere toward Rhea. Analysis of two other snapshots of multicomponent waveforms, recorded in the Rhea magnetic flux tube, shows whistler-mode waves with the same properties but with weaker intensities. Interestingly enough, one additional snapshot recorded after Cassini left the Rhea magnetic flux tube still shows intense whistler-mode waves with the same properties (Figure 4, right).

[12] The absorption of electrons by Rhea generates an unusually strong temperature anisotropy which is known to cause the first order cyclotron instabilities leading to emission of the whistler-mode waves. The $v_\parallel$ - dependent anisotropy values can be obtained using the definition of *Kennel and Petschek* [1966],

$$A(v_\parallel) = \int (v_\parallel \partial f/\partial v_\perp - v_\perp \partial f/\partial v_\parallel) v_\perp^2/v_\parallel \, d\, v_\perp \Big/ \int 2 f \, v_\perp d\, v_\perp \tag{4}$$

Figure 2g shows that $A(v_\parallel)$ peaks at a value of ~6 for $v_\parallel = v_{\parallel A} \sim -0.03c$. The region of $A(v_\parallel) > 1$ extends to $v_\parallel \sim -0.1c$.

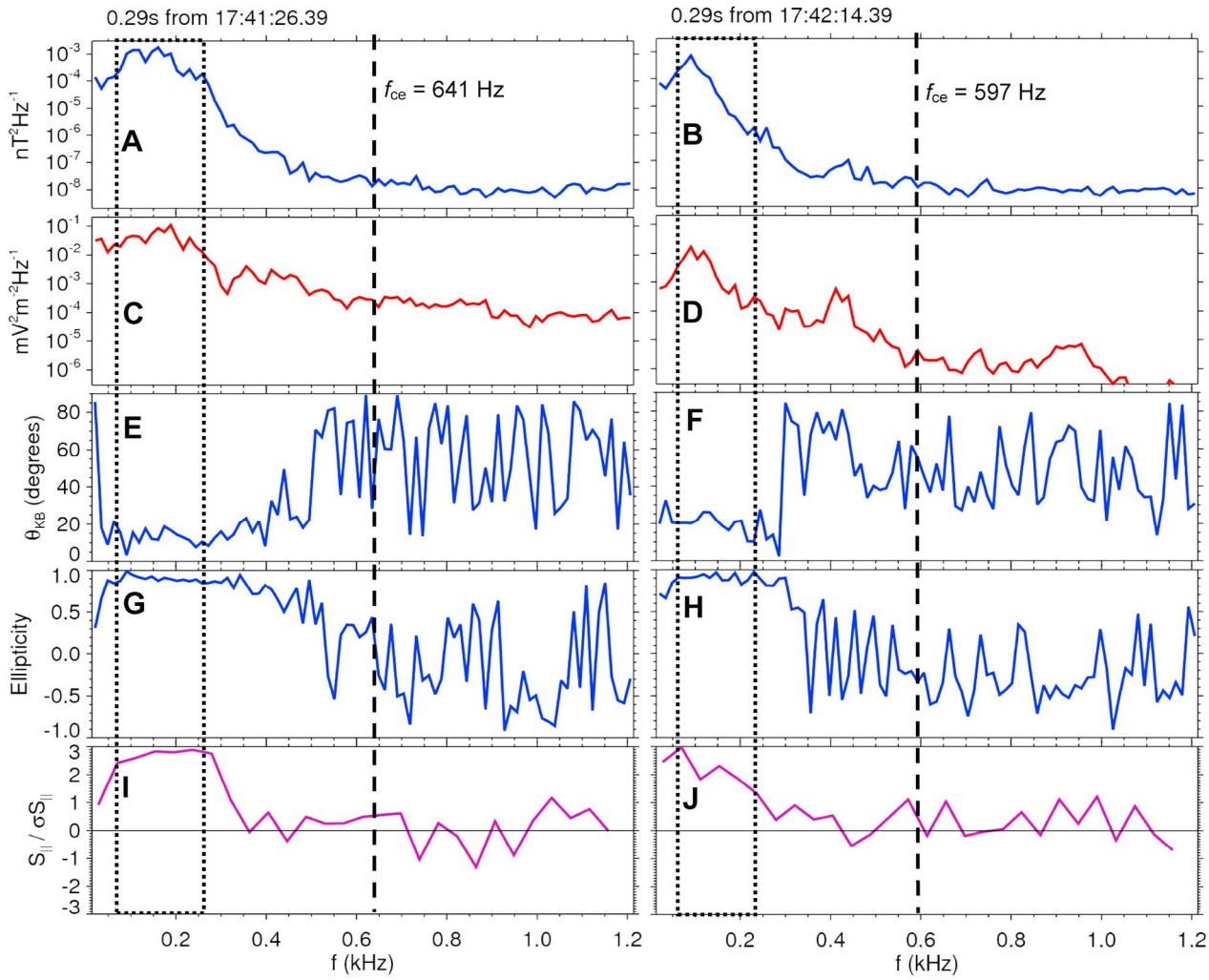

Figure 4. Results of frequency-dependent propagation and polarization analysis of two neighboring snapshots of multi-component waveforms recorded on March 2, 2010 (left) from 17:41:26.39 UT – inside the Rhea flux tube, and (right) from 17:42:14.39 UT – outside the Rhea flux tube. (a, b) Sum of power-spectral densities from the three orthogonal magnetic components; (c, d) Sum of power spectral densities from two electric components; (e, f) Angle between the wave vector direction and $\mathbf{B_0}$. (g, h) Ellipticity obtained as the ratio of the two largest axes of the magnetic-field polarization ellipsoid with the sign reflecting the sense of polarization. (i, j) Component of the Poynting vector along $\mathbf{B_0}$ normalized by the estimated uncertainty of the analysis method.

In other intervals of $v_{||}$ the anisotropy is close to zero. The parallel wave numbers unstable to the first order cyclotron resonance for $v_{||} = v_{||A}$ are

$$k_{||A} = 2\pi(f - f_{ce})/v_{||A}, \quad (5)$$

where f_{ce} is the electron cyclotron frequency.

[13] With f_{ce} = 630 Hz at the time of measurement of the electron phase space densities, and assuming $f \sim 0.3\ f_{ce}$ (according to Figure 4a) we obtain an unstable parallel wave number of $k_{||A} \sim 3 \times 10^{-4}$ m^{-1}. This value exactly corresponds to the value obtained from the whistler-mode dispersion relation for this frequency. In other words, for the observed frequencies of the whistler mode waves, the parallel cyclotron resonance energy would be in the unstable region around 230 eV. An estimate of the linear growth rate of whistler-mode waves, according to *Kennel and Petschek* [1966] is

$$\gamma/f_{ce} = \pi\,\eta(v_{||A})[1 - f/f_{ce}]^2[A(v_{||A}) - f/(f_{ce} - f)]. \quad (6)$$

With a roughly estimated plasma density of $n \sim 4$ cm^{-3}, based on the observations of the bursty plasma waves centered at a frequency of $f_p \sim 18$ kHz, with $F(v_{||A}) \sim 2 \times 10^{-4}$ m^{-4}s from Figure 2i, and with the fraction of resonant hot electrons $\eta(v_{||A}) = v_{||A}\ F(v_{||A})/n \sim 4.5 \times 10^{-4}$, we obtain a growth rate of $\gamma/f_{ce} \sim 4 \times 10^{-3}$. Note that, unlike the Landau instability described in equation (2), the cyclotron instability in equation (5) generates, for the unstable features with $v_{||A} < 0$ (i.e., in the direction from Rhea) waves propagating with positive $k_{||}$ (i.e., from the Saturn's magnetosphere toward Rhea). The measurement of the sign of the parallel component of the Poynting flux in Figure 4i

shows that the observed whistler-mode waves propagate toward Rhea. Note also, that the observed whistler-mode waves are the only electromagnetic waves observed in the Rhea flux tube. They can propagate large distances along the flux tube toward Rhea. Their group speed is directed approximately along the magnetic field line. The small but finite group velocity angles with respect to the magnetic field line cause these waves to be slightly spread outside the flux tube.

[14] Very high amplitudes of whistler-mode waves (more than 2% of the ambient magnetic field - see Figures 1f and 1g) would likely lead to nonlinear interactions with energetic electrons. Similar but relatively weaker emissions of whistler-mode chorus in the Earth's magnetosphere are known to cause pitch angle diffusion of energetic electrons [*Ni et al.*, 2008] and their precipitation into the atmosphere [*Nishimura et al.*, 2010], acting at similar spatial scales [*Bortnik et al.*, 2008]. The empty slot region in the radiation belts is also attributed to whistler-mode waves [*Bortnik et al.*, 2009]. We propose that strong whistler-mode waves which can propagate from large distances in the vicinity of the Rhea flux tube can act by a similar mechanism, effectively decreasing the flux of energetic electrons and thus possibly explaining the observed depletion of energetic electrons in the moon's vicinity [*Jones et al.*, 2008]. A depletion of energetic electrons is indeed observed by Cassini also in this case (E. Roussos et al., manuscript in preparation, 2011).

[15] The observed large intensities of whistler-mode waves suggest that their amplitudes have been amplified by a factor of ~10^5 from the background noise detected at these frequencies outside the Rhea flux tube. The whistler mode group speed at a frequency of 0.3 f_{ce} is approximately $v_G \sim 6 \times 10^6$ m s^{-1} (i.e., $v_G \sim 0.02$ c). This, together with the above discussed growth rate, gives the characteristic e-folding scale of the linear convective growth of $L_e = v_G/(2\pi\gamma) \sim 380$ km. The characteristic length necessary to amplify the waves to the observed amplitudes is then very short compared to the scale of the Saturn's magnetosphere, $L = L_e \ln(10^5) \sim 4400$ km. This length, however, is probably unrealistically short and a larger amplification region would be necessary in reality. The unstable features of the observed phase space density (its large anisotropy) are likely to be the strongest at the point of observation close to Rhea and they will weaken with the distance from the moon. The growth rates will be therefore lower further out from Rhea and the waves may need somewhat larger lengths to be amplified to the observed amplitudes.

[16] Understanding generation and effects of these intense plasma waves is important not just to Rhea, and not just to Saturn but to all planetary magnetospheres. This also includes the Earth's magnetosphere, where intense whistler-mode chorus waves have been shown to contribute to both loss and acceleration [*Bortnik et al.*, 2008, 2009] of relativistic electrons in the outer Van Allen radiation belt.

[17] **Acknowledgments.** Cassini-Huygens is a mission of international collaboration between NASA, the European Space Agency (ESA), and the Agenzia Spaziale Italiana (ASI). The research at the University of Iowa was supported by NASA through contract 1415150 with the Jet Propulsion Laboratory. O.S. acknowledges additional support from grants CACR P205-10-2279, ME10001, and LH11122. G.H.J. is supported by a UK STFC Advanced Fellowship. Cassini work at MSSL-UCL is supported by STFC, the UK Space Agency, and ESA.

[18] The Editor thanks one anonymous reviewer for his//her assistance in evaluating this paper.

References

Bortnik, J., R. M. Thorne, and U. S. Inan (2008), Nonlinear interaction of energetic electrons with large amplitude chorus, *Geophys. Res. Lett.*, *35*, L21102, doi:10.1029/2008GL035500.

Bortnik, J., et al. (2009), An observation linking the origin of plasmaspheric hiss to discrete chorus emissions, *Science*, *324*, 775–778, doi:10.1126/science.1171273.

Dougherty, M. K., et al. (2004), The Cassini magnetic field investigation, *Space Sci. Rev.*, *114*, 331–383, doi:10.1007/s11214-004-1432-2.

Gurnett, D. A., and A. Bhattacharjee (2005), *Introduction to Plasma Physics*, Cambridge Univ. Press, Cambridge, U. K.

Gurnett, D. A., G. B. Hospodarsky, W. S. Kurth, D. J. Williams, and S. J. Bolton (1993), Fine structure of Langmuir waves produced by a solar electron event, *J. Geophys. Res.*, *98*, 5631–5637, doi:10.1029/92JA02838.

Gurnett, D. A., et al. (2004), The Cassini radio and plasma wave investigation, *Space Sci. Rev.*, *114*, 395–463, doi:10.1007/s11214-004-1434-0.

Horne, R. B., et al. (2005), Wave acceleration of electrons in the Van Allen radiation belts, *Nature*, *437*, 227–230, doi:10.1038/nature03939.

Jones, G. H., et al. (2008), The dust halo of Saturn's largest icy moon, Rhea, *Science*, *319*, 1380–1384, doi:10.1126/science.1151524.

Kennel, C. F., and H. E. Petschek (1966), Limit on stably trapped particle fluxes, *J. Geophys. Res.*, *71*, 1–28.

Khurana, K. K., C. T. Russell, and M. K. Dougherty (2008), Magnetic portraits of Tethys and Rhea, *Icarus*, *193*, 465–474, doi:10.1016/j.icarus.2007.08.005.

Lin, R. P., et al. (1986), Evidence for nonlinear wave-wave interactions in solar type III radio bursts, *Astrophys. J.*, *308*, 954–965, doi:10.1086/164563.

Ni, B., R. M. Thorne, Y. Y. Shprits, and J. Bortnik (2008), Resonant scattering of plasma sheet electrons by whistler-mode chorus: Contribution to diffuse auroral precipitation, *Geophys. Res. Lett.*, *35*, L11106, doi:10.1029/2008GL034032.

Nishimura, Y., et al. (2010), Identifying the driver of pulsating aurora, *Science*, *330*, 81–84, doi:10.1126/science.1193186.

Pitman, K. M., et al. (2008), First high solar phase angle observations of Rhea using Cassini VIMS: Upper limits on water vapor and geologic activity, *Astrophys. J.*, *680*, L65–L68, doi:10.1086/589745.

Reiner, M. J., et al. (1995), Ulysses/Galileo observations of type III radio bursts and associated in-situ electrons and Langmuir waves, *Space Sci. Rev.*, *72*, 261–266, doi:10.1007/BF00768789.

Robinson, P. A., A. J. Willes, and I. H. Cairns (1993), Dynamics of Langmuir and ion-sound waves in type III solar radio sources, *Astrophys. J.*, *408*, 720–734, doi:10.1086/172632.

Santolík, O., F. Lefeuvre, M. Parrot, and J. L. Rauch (2001), Complete wave-vector directions of electromagnetic emissions: Application to INTERBALL-2 measurements in the nightside auroral zone, *J. Geophys. Res.*, *106*, 13,191–13,201, doi:10.1029/2000JA000275.

Santolík, O., M. Parrot, and F. Lefeuvre (2003), Singular value decomposition methods for wave propagation analysis, *Radio Sci.*, *38*(1), 1010, doi:10.1029/2000RS002523.

Teolis, B. D., et al. (2010), Cassini finds an oxygen-carbon dioxide atmosphere at Saturn's icy moon Rhea, *Science*, *330*, 1813–1815, doi:10.1126/science.bkek1198366.

Tiscareno, M. S., J. A. Burns, J. N. Cuzzi, and M. M. Hedman (2010), Cassini imaging search rules out rings around Rhea, *Geophys. Res. Lett.*, *37*, L14205, doi:10.1029/2010GL043663.

Wilson, R. J., R. L. Tokar, W. S. Kurth, and A. M. Persoon (2010), Properties of the thermal ion plasma near Rhea as measured by the Cassini plasma spectrometer, *J. Geophys. Res.*, *115*, A05201, doi:10.1029/2009JA014679.

Young, D. T., et al. (2004), Cassini plasma spectrometer investigation, *Space Sci. Rev.*, *114*, 1–112, doi:10.1007/s11214-004-1406-4.

F. J. Crary, Southwest Research Institute, PO Drawer 28510, San Antonio, TX 78229, USA.

M. K. Dougherty, Blackett Laboratory, Imperial College London, Exhibition Road, London SW7 2BZ, UK.

D. A. Gurnett, G. B. Hospodarsky, W. S. Kurth, J. S. Leisner, and P. Schippers, Department of Physics and Astronomy, University of Iowa, Iowa City, IA 52242-1479, USA.

G. H. Jones, Mullard Space Science Laboratory, University College London, Holmbury St. Mary RH5 6NT, UK.

C. T. Russell, Institute of Geophysics and Planetary Physics, University of California, 603 Charles Young Dr. East, 3845 Slichter Hall, Los Angeles, CA 90095-1567, USA.

O. Santolík, Faculty of Mathematics and Physics, Charles University, V Holesovickach 2, Prague 8 18000, Czech Republic. (ondrej.santolik@mff.cuni.cz)